Available online at www.sciencedirect.com

SCIENCE DIRECT

Thermochimica Acta 447 (2006) 147–153

thermochimica acta

www.elsevier.com/locate/tca

Decomposing or subliming? An investigation of thermal behavior of L-leucine

Jie Li[a], Zhiyong Wang[a], Xi Yang[a], Ling Hu[a], Yuwen Liu[a,b,*], Cunxin Wang[a]

[a] *College of Chemistry and Molecular Science, Wuhan University, Wuhan 430072, Hubei, China*
[b] *College of Live Science, Wuhan University, Wuhan 430072, China*

Received 20 December 2005; received in revised form 8 May 2006; accepted 8 May 2006
Available online 16 May 2006

Abstract

The thermal behavior of L-leucine under inert conditions was investigated by TGA, FTIR and TG–FTIR. The TG results showed that only one mass loss stage of more than 99% happened when L-leucine was under program heating with temperature ranging from 30 to 600 °C. The apparent activation energy, pre-exponential factor and the most probable model function were obtained by using of master plots method. The results of kinetic study showed that the decrease in mass of L-leucine was due to subliming rather than decomposing. And this was proved by the FTIR spectrum analysis and the directly observed subliming phenomenon. The results of TG–FTIR experiments showed that there was only one stage of decomposition process that happened after the subliming of leucine. The gas products were CO_2, NH_3, CO and some organic compounds such as 3-methyl-1-butanamine, and the main primary decomposition was decarboxylation.

Keywords: L-Leucine; Thermal decomposition; Subliming; Thermogravimetry; TG–FTIR

1. Introduction

Due to their crucial biological importance, amino acids have remained a classic subject for pyrolytic studies for decades [1–18]. Many techniques, such as UV [14,16], IR [3,5,8], Raman [8], NMR [3,17], HPLC [13,14,16], GC–MS [1,3,4,6,15,17,18], GC–FTIR–MS [13,16], TG [17], DSC [9] and TG–DSC [10–12] have been used to identify the products and the mechanisms of their thermal decomposition. Now it is well known that their decomposition products are mainly simple inorganic compounds (CO_2, H_2O, NH_3 and CO), with a variety of volatile organic compounds (amines, nitriles, amides, hydrocarbons, etc.) and some less-volatile organic compounds (piperazine-2,5-diones and other complex cyclic compounds). The thermal fragmentations of various amino acids are considered as very complicated processes, which involved many pathways such as decarboxylation, deamination, dehydration and condensation reactions.

The former thermogravimetry research [10–12] of amino acids showed an interesting phenomenon. Firstly, the TG curves of most amino acids have multiple mass loss stages, while those of the aliphatic α-amino acids have only one mass loss stage except for glycine. Secondly, most amino acids lost only partial mass even at 600 °C, while the aliphatic amino acids lost mass completely below 400 °C. As we known, the decomposition of amino acids is a complicated process. So it is easy for us to understand why the TG curves of most amino acids exhibit a multistage decomposing process. But for the aliphatic α-amino acids, single-stage decomposition results seem to be abnormal and worthy of investigating.

Although lots of articles have been published on the experimental and mechanistic aspects of amino acids pyrolysis, little information is available on the kinetic aspects of these processes. And the kinetic studies reported were very simple, in which a 1st order chemical reaction model was used arbitrarily [10–12]. A more precise kinetic method should be used to investigate their thermal behavior.

The thermal decomposition mechanism was investigated based upon off-line products detection in previous studies. By using such methods as MS technique, products of different

---

[*] Corresponding author. Tel.: +86 27 87218614; fax: +86 27 68754067.
E-mail address: ipc@whu.edu.cn (Y. Liu).

0040-6031/$ – see front matter © 2006 Elsevier B.V. All rights reserved.
doi:10.1016/j.tca.2006.05.004

reaction steps will mix together, and cannot provide much information about the sequences these reactions. In present work, the TG–FTIR technique, which can conduct simultaneous and continuous real time analysis [19–23], is used. It can provide more information about the reaction sequences and the relevant products.

This paper is focused on the kinetic analysis of the thermal behavior of L-leucine under programming heating. The "kinetic triplet": apparent activation energy, pre-exponential factor and the most probable model function were obtained by the iso-conversional method and the master plots method. And the TG–FTIR technique was used to monitor the decomposition processes online. The results show that when L-leucine is heated, it sublimes and then decomposes in gas phase. The mass loses in TG measurement is caused by the subliming of L-leucine.

2. Theoretical

For a reaction under non-isothermal condition, its kinetic function can be described as the following form:

$$g(\alpha) = \frac{AE_a}{\beta R} P(u) \tag{1}$$

where α is the extent of conversion, β the heating rate, E_a the apparent activation energy, R the gas constant, A is pre-exponential factor, $g(\alpha)$ is the integral expression of kinetic model function, and $P(u) = \int_{\infty}^{u} -(e^u/u^2)\,du, \quad u = E_a/RT$.

Because the exponential integral, $P(u)$, has no analytical solution. An approximation formula of high accuracy [24] was used.

$$-\ln P(u) = 0.37773896 + 1.89466100 \ln u + 1.00145033u \tag{2}$$

Inserting Eq. (2) into Eq. (1), one can obtain:

$$\ln\left[\frac{\beta}{T^{1.89466100}}\right] = \left[\ln\frac{AE_a}{Rg(\alpha)} + 3.63504095 - 1.89466100 \ln E_a\right] - 1.00145033\frac{E_a}{RT} \tag{3}$$

The first term at the right side of Eq. (3) is a constant corresponding to a given value of α. So for a series of experiments at different heating rates, the plot of $\ln(\beta/T^{1.89466100})$ versus $1/T$ with the same conversional ratio should be a line with the slope of $-1.00145033\,E_a/R$. Then, the apparent activation energy E_a can be calculated from the slope.

Inserting $\alpha = 0.5$ into Eq. (1), one can get:

$$g(0.5) = \frac{AE_a}{\beta R} P(u_{0.5}) \tag{4}$$

where $u_{0.5} = E_a/RT_{0.5}$, $T_{0.5}$ is the temperature when α equals to 0.5. When Eq. (1) is divided by Eq. (4), the following equation is obtained:

$$\frac{g(\alpha)}{g(0.5)} = \frac{P(u)}{P(u_{0.5})} \tag{5}$$

By plotting $g(\alpha)/g(0.5)$ against α according to different theoretical model functions, the theoretical master plots can be obtained for different kinetic mechanisms. With E_a calculated from Eq. (3), the experimental master plots of $P(u)/P(u_{0.5})$ against α could be drawn from the experimental data obtained under different heating rates. Eq. (5) indicates that, for arbitrary α, the experimental value of $P(u)/P(u_{0.5})$ and theoretically calculated values of $g(\alpha)/g(0.5)$ are equivalent when an appropriate kinetic model is used. So this integral master plots method can be used to determine the reaction kinetic models of non-isothermal reactions.

Then, the pre-exponential factor A can be estimated form the slope of the plot of $g(\alpha)$ versus $E_aP(u)/\beta R$.

3. Experimental

Commercially available L-leucine (Analytical Grade, Duchefa) was used without further purification.

TG measurements were performed on a Setaram Setsys 16 TG–DTA/DSC Instrument, France. Instrument calibration was performed with standard indium, tin, lead, zinc, silver and gold samples of known melting temperature. All standards were of purity >99.99%. For the kinetics measurements, about 5 mg sample was weighted into an open alumina crucible. The furnace temperature was programmed to rise from ambient temperature to 600 °C linearly at the rates of 2, 5, 10, 15 and 20 K min^{-1}. The reaction atmosphere was nitrogen gas of high purity (≥99.999%) with a flow rate of 50 ml min^{-1}.

The subliming detection was carried out in a beaker full of N_2. About 1 g L-leucine was used in this experiment. Lots of white solid condensate was collected. FTIR measurements of both the condensate and pure L-leucine were carried out with a Thermo Nicolet 360 Fourier Transform Infrared Spectrometer. The data was collected at a resolution of 4 cm^{-1} in the range 4000–400 cm^{-1} using KBr pellet technique.

The TG–FTIR system composed of the Setaram Setsys 16 TG–DTA/DSC Instrument and a Thermo Nicolet Nexus 670 Fourier Transform Infrared Spectrometer. For TG–FTIR measuring, about 10 mg sample was weighted into an open alumina crucible. The heating rate of the TG furnace was 20 K min^{-1}, and nitrogen gas of high purity (≥99.999%) with a flow rate of 100 ml min^{-1} was used as carrier gas. The sample was heated from ambient temperature to 600 °C. The transfer line used to connect TG and FTIR was a 1 m long stainless steel tube with an internal diameter of 2 mm, of which the temperature is maintained at 200 °C. The TGA accessory of the IR Spectrometer was used, in which the 45 ml gas cell with a 200 mm path length was also heated at a constant temperature of 200 °C. The IR spectra were collected at 8 cm^{-1} resolution, co-adding 8 scans per spectrum. This resulted in a temporal resolution of 4.32 s. Lag time that the gas products went from furnace to gas cell was about 7 s. The FTIR spectra have been identified based on the FTIR reference spectra available on the World Wide Web in the public spectrum libraries of NIST [25] and SADTLER Standard Infrared Spectra [26].

4. Results and discussion

4.1. The result of thermal kinetics analysis

TG curves corresponding to the thermal mass-loss process of L-leucine at five different heating rates 2, 5, 10, 15, and 20 K min^{-1} are shown in Fig. 1. The thermal behavior of L-leucine is characterized by a single stage with mass percent loss (mass%) of almost 100% at 207–355 °C.

The values of α among 0.2–0.8 with an increment of 0.05 were chosen for kinetic calculation. Plotting $\ln(\beta/T^{1.89466100})$ against $1/T$ using a linear regressive of least-square method, we got the values of E_a at different conversions which were listed in Table 1. As shown in Table 1, all these plots had linear correlation coefficients larger than 0.99. The apparent activation energy did not vary with the increase of conversion ratios and the average value is 137.95 ± 2.66 kJ mol^{-1}. This value is very close to the literature values of 129.91 kJ mol^{-1} [10] and 135 kJ mol^{-1} [11,12]. Little dependence of the activation energy on the extent of conversion suggests that the reaction took place through a single-step reaction mechanism.

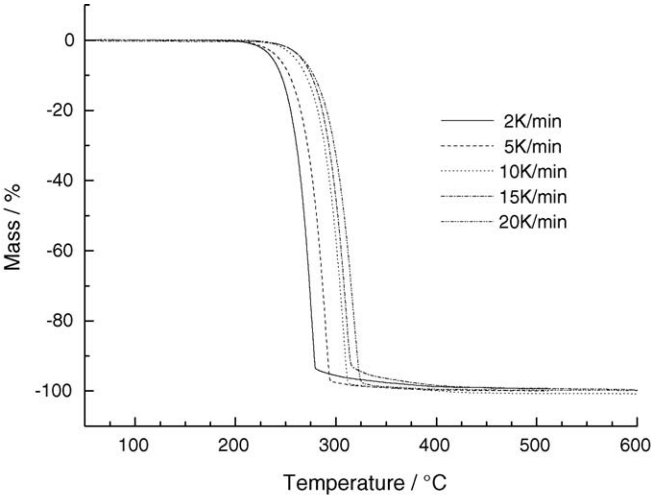

Fig. 1. TG curves of L-leucine at different heating rate, N_2 flow rate 50 ml/min.

Table 1
The apparent activation energy E_a and the correlation coefficients r of linear regress at different conversions α

α	E_a/kJ mol^{-1}	r
0.20	143.03	0.9905
0.25	140.57	0.9919
0.30	139.84	0.9923
0.35	139.40	0.9927
0.40	139.11	0.9927
0.45	138.91	0.9936
0.50	138.74	0.9935
0.55	137.64	0.9941
0.60	137.06	0.9941
0.65	136.20	0.9943
0.70	134.36	0.9938
0.75	134.32	0.9938
0.80	134.20	0.9942

Table 2
The 40 model functions for the determination of the most probably model function

No.	$g(\alpha)$	Reaction type
1	α^2	
2	$\alpha + (1-\alpha)\ln(1-\alpha)$	
3–6	$(1-(1-\alpha)^n)^m$, $n = 1/2, 1/3$; $m = 1/2, 2$	Diffusion
7	$1 - 2/3\alpha - (1-\alpha)^{2/3}$	
8	$((1+\alpha)^{1/3} - 1)^2$	
9	$((1-\alpha)^{-1/3} - 1)^2$	
10–20	$-\ln(1-\alpha)^n$, $n = 1/4, 1/3, 2/5, 1/2, 2/3, 3/4, 1, 3/2, 2, 3, 4$	Nucleation and nucleus growth
21–25	α^n, $n = 1/4, 1/3, 1/2, 3/2, 2$	Power law
26	α	Phase boundary reaction
27–31	$m(1-(1-\alpha)^n)$, $(m, n) = (1,1/4), (1,1/3), (3,1/3), (1,1/2), (2,1/2)$	
32–34	$1-(1-\alpha)^n$, $n = 2, 3, 4$	Chemical reaction order
35–37	$(1-\alpha)^n$, $n = -1, -1/2, -2$	
38	$(1-\alpha)^{-1}-1$	
39–40	$\ln(\alpha^n)$, $n = 1, 2$	Exponent law

To determine the most probable mechanism, 40 basic model functions in Table 2 were tested. According to the value of E_a, the theoretical master plots of $g(\alpha)/g(0.5)$ versus α and the experimental master plots of $P(u)/P(u_{0.5})$ versus α were obtained, as shown in Fig. 2. The superposition of experiment master plots at different heating rates indicates that the kinetics process of thermal mass loss of L-leucine can be described by a single model function. It can be easily seen from Fig. 2 that the most probable model function is the No. 26 function, $g(\alpha) = \alpha$, which is used to describe one-dimensional phase boundary reaction. This result indicates that it is improper to use the 1st order reaction model function for the kinetics calculation as done in literatures [10–12].

By plotting $g(\alpha)$ against $E_aP(u)/\beta R$ at different heating rate (shown in Fig. 3), the pre-exponential factor $\ln A = 23.83 \pm 0.10$ is obtained. This value is different from the literature values of

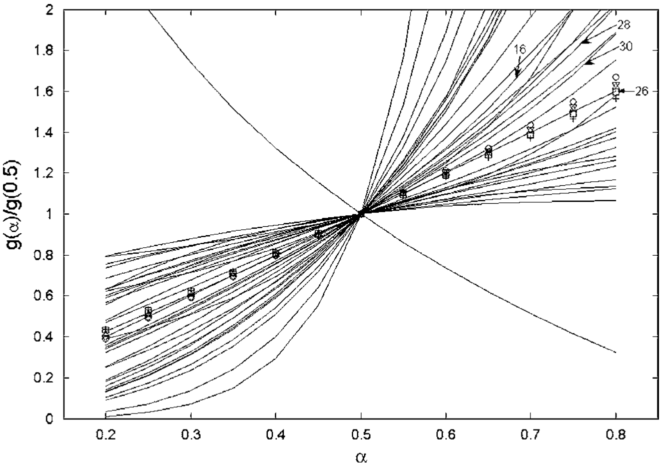

Fig. 2. The theoretical master plots (—) and the experimental master plots at heating rates of 2 K/min(+), 5 K/min(▽), 10 K/min(△), 15 K/min(□) and 20 K/min(○). Models that have been used to describe the sublimation process are labeled as: (16) 1st order reaction model; (26) one-dimensional phase boundary model; (28) three-dimensional phase boundary model: contracting sphere; (30) two-dimensional phase boundary model: contracting cylinder.

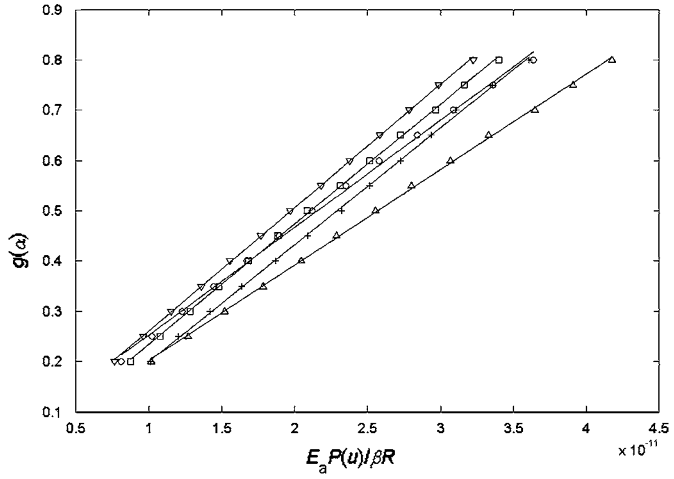

Fig. 3. The curves of $g(\alpha)$ against $E_aP(u)/\beta R$ at the heating rate of 20 K/min(◯), 15 K/min(□), 10 K/min(△), 5 K/min(▽), 2 K/min(+) and the result of linear fitting (−).

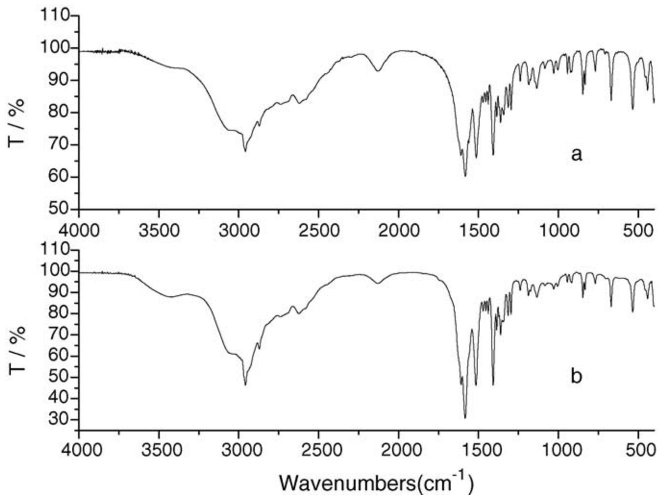

Fig. 4. The FTIR spectrums of the pure L-leucine and the solid condensate gotten by the subliming experiment: (a) the FTIR spectrum of pure Leu; (b) the FTIR spectrum of solid condensate.

26.26 [10] and 27.4 [11,12]. This difference is mainly caused by the different model function used, which could affect the value of the pre-exponential factor remarkably.

4.2. *The result of subliming detection*

According to the result of kinetic analysis, the whole mass loss process of leucine abides the single step reaction mechanism. And the one-dimensional phase boundary model is satisfied with this mechanism. As we know, this model is used to describe the reaction whose rate is proportional to the surface area of the interface. With consideration of the nearly 100% mass loss, we believe that the process is the subliming process of leucine.

The subliming detection was carried out to verify this postulation. L-Leucine at the bottom of the beaker disappeared completely when heated, and white solid can bee seen condensed where the gas was cooled. The IR spectrum of the solid condensate is the same as that of L-leucine (shown in Fig. 4). This indicated that the condensate is pure L-leucine and not contains the decomposition products. This experiment shows that leucine will sublime when heated.

4.3. *Evolved gas analysis by online-coupled TG–FTIR*

Identity and evolution dynamics of the evolved gaseous species from thermo gravimetric apparatus have been described by means of online-coupled FTIR. With consideration of the lag time from furnace to gas cell, the DTG curve and the Gram–Schmidt curve are shown in Fig. 5. Both of them have only one peak. It can be easily seen that the peak of Gram–Schmidt curve is at higher temperature than that of the DTG curve. And the onset point of Gram–Schmidt curve is 302.56 °C, which is also higher than the onset point of the DTG curve, 294.66 °C. This result indicates that for L-leucine, the mass loss process and thermal decomposition process do not take place simultaneously. The mass loss process takes place earlier than decomposition. With consideration of the results of kinetics analysis and sublime detection, it can be concluded that the mass loss in TG detection is caused by subliming of leucine.

So we propose that the L-leucine sublimes at 294.66 °C and the decomposition of the gaseous leucine takes place at 302.56 °C. This phenomenon could not be noticed by researchers merely using TG measurements [10–12], for TG alone cannot distinguish between subliming and decomposing. And for the researches done by GC–MS, due to the fast heating rates used, which were 50–80 °C/s [1,3,4,6,15,17,18] typically, the tiny difference between subliming temperature and decomposition temperature can hardly be noticed.

The IR absorption spectra of the evolved gases at different time are shown in Fig. 6. And a typical spectrum obtained at 346.15 °C is shown in Fig. 7. From this figure, three small molecular inorganic gaseous species, CO_2, NH_3 and CO, are easily identified by their characteristic peaks: carbon dioxide at 2361 cm^{-1}; ammonia at 965, 930 cm^{-1}; carbon monoxide at

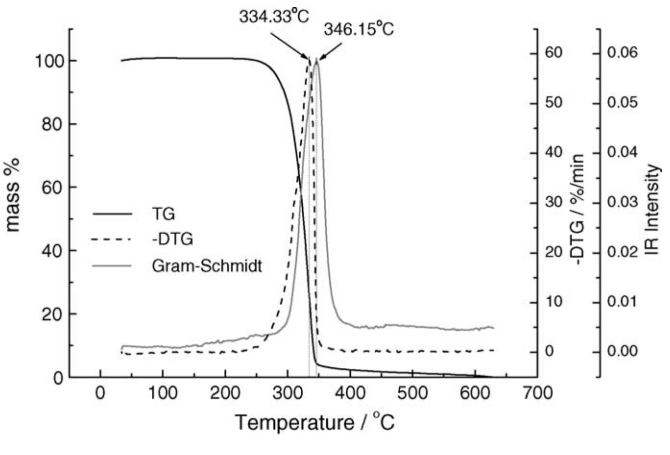

Fig. 5. The curves of TG, DTG and the Gram–Schmidt of evolved gases, gotten during the leucine pyrolysis process by TG–FTIR, heating rate 20 K/min, N_2 flow rate 100 ml/min.

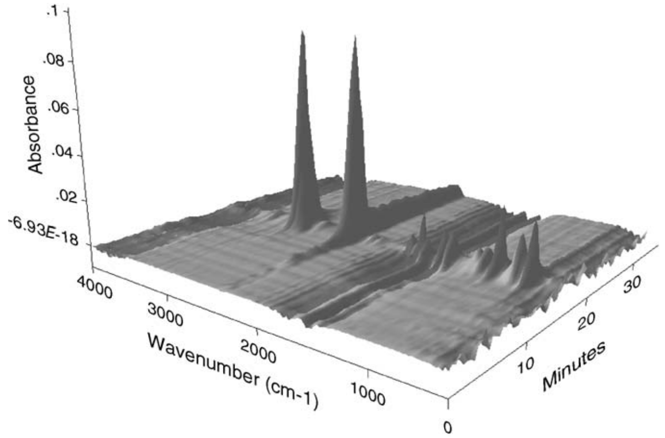

Fig. 6. The 3D surface graph for the FTIR spectra of the evolved gases produced by L-leucine pyrolysis (heating rate 20 K/min; N_2 flow rate 100 ml/min).

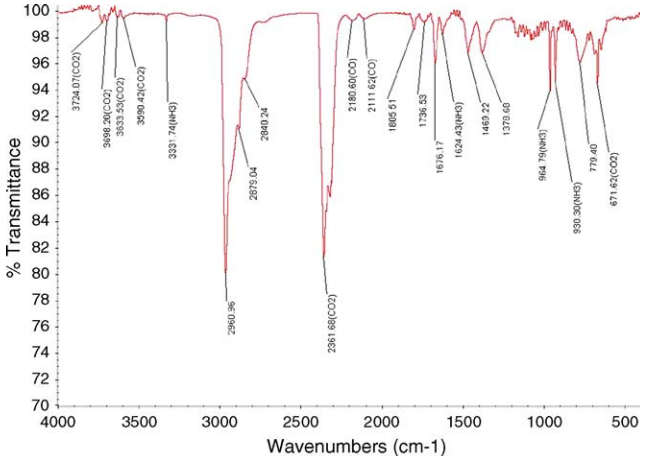

Fig. 7. FTIR spectrum of evolved gases from L-leucine decomposed in N_2, measured at 346.15 °C by online-coupled TG–FTIR (heating rate 20 K/min; N_2 flow rate 100 ml/min).

2181, 2112 cm^{-1}. And the quantity of CO_2 is much larger than that of the other two species.

The organic gaseous species are complex. The IR absorption in the 1600–1800 cm^{-1} region gives the presence of several different C=O groups, which indicates that esters (1805 cm^{-1}), aldehydes (2728 cm^{-1}, 1736 cm^{-1}), acidamides (1676 cm^{-1}) and amines (1624 cm^{-1}) exist in the evolved gas. The strong absorption of CO_2 means that the reaction of decarboxylating to yield 3-methyl-1-butanamine is the main primary decomposition reaction. The existence of 3-methyl-1-butanamine can be ascertained by appropriately relative absorption intensity of IR absorption peaks in the Fig. 6: $\nu_{C–H}$ 2850–2960 cm^{-1}, $\delta_{C–H}$ 1469 cm^{-1}, 1379 cm^{-1}, $\delta_{N–H}$ 1624 cm^{-1}, $\nu_{C–N}$ 1069 cm^{-1}, and $\delta_{N–H}$ 780 cm^{-1}. This result is consistent with Simmond's report [3]. And it is difficult to identify esters, aldehydes and acidamides for their weak IR absorption.

Nitriles and alkenes as products of pyrolysis of leucine have been verified by GC–MS [3,4]. But in our experiment, the absence of IR absorption of C≡N stretch region, which is about 2250 cm^{-1}, indicates the absence of nitriles. And no absorption in the region of 3100–3000 cm^{-1} gives the absence of the C=C group. We believe these were caused by their low concentrations. Although the absorbance in the C–H stretch region of 2960–2800 cm^{-1} is very strong, the existence of alkanes cannot be ascertained for most of organic compounds exhibit absorbance in this region.

The plots of IR absorbance at several characteristic wavenumbers versus temperature are shown in Fig. 8. These curves indicate the evolution rates versus temperature for each gaseous product. The peak temperatures, which represent the temperature of the maximum evolution rate, show that the release of CO_2 is a little earlier than the other gaseous products. And in the evolved gases, amine was detected in large quantities. All these indicate that the decarboxylating is the main primary step in thermal decomposition of leucine. It is well known that amino acid can exist in a Zwitterion form,

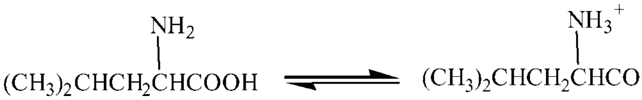

$$(CH_3)_2CHCH_2\overset{\overset{NH_2}{|}}{C}HCOOH \rightleftharpoons (CH_3)_2CHCH_2\overset{\overset{NH_3^{+}}{|}}{C}HCOO^{-}$$

and we think that is why decarboxylation is greatly favored for the aliphatic α-amino acids. We suggest that the following reactions may be included in the thermal decomposition of L-leucine with consideration of Simmond's report [3,4].

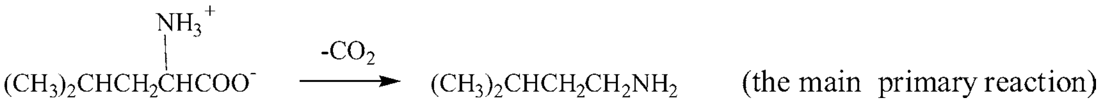

$$(CH_3)_2CHCH_2\overset{\overset{NH_3^{+}}{|}}{C}HCOO^{-} \xrightarrow{-CO_2} (CH_3)_2CHCH_2CH_2NH_2 \quad \text{(the main primary reaction)} \qquad (1)$$

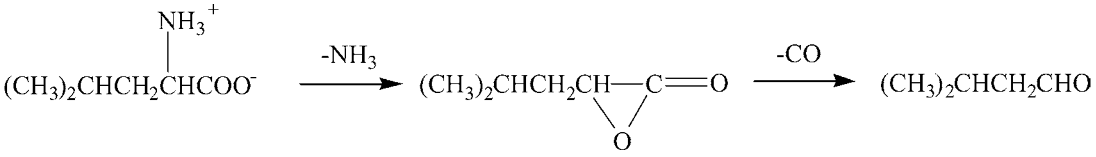

(2)

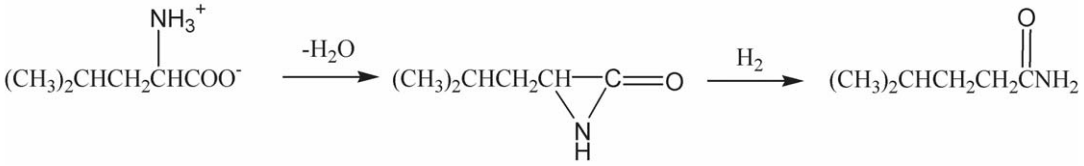

(3)

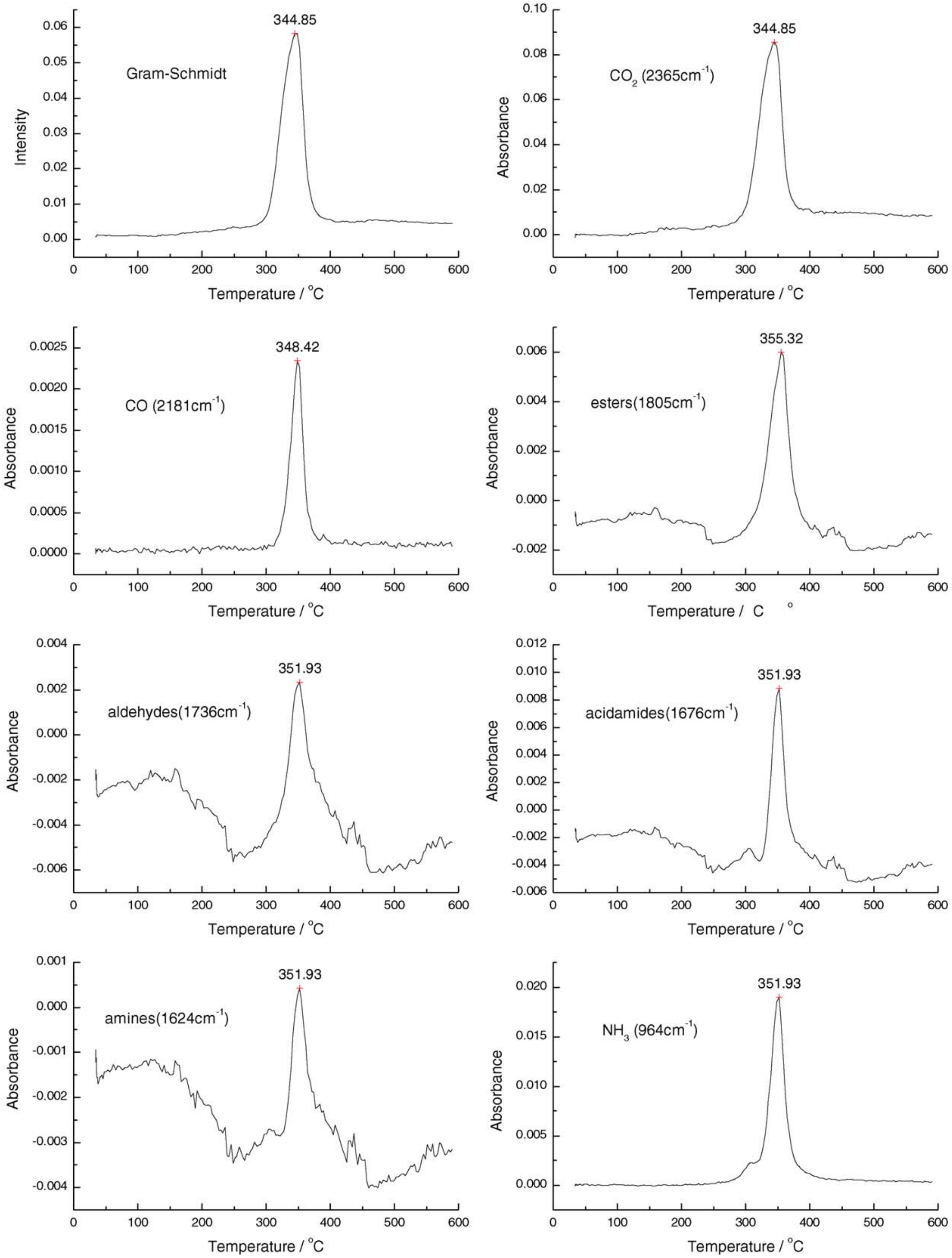

Fig. 8. Absorbance at different wave numbers vs. temperature curves of evolved gases from L-leucine decomposed in N_2, measured by online-coupled TG–FTIR (heating rate 20 K/min; N_2 flow rate 100 ml/min).

5. Conclusions

When heated, solid L-leucine begins to sublime at 294 °C and then decomposes in gas phase. The mass decrease in TG measurement is caused by subliming, not decomposition. The decomposition temperature of leucine is higher than its subliming temperature. The TG–FTIR study shows that the main gaseous products are CO_2, NH_3, CO, 3-methyl-1-butanamine and some other organic compounds. The decomposition process of L-leucine includes decarboxylation, deamination, dehydration and some other reactions. The decarboxylation is believed as the main primary reaction.

This work indicates that the thermogravimetric analysis cannot be used to distinguish between subliming and decomposing because the mass loss happens in both of the two processes. A detailed research needs the combined using of more specific techniques such as IR or MS.

The kinetic analysis of TG curves in this paper does not follow rigorously 1st order kinetic model. And the kinetic triplets were obtained by iso-conversional method and the master plots method. The present work proves that the one-dimensional phase boundary reaction can fit the kinetic data better than the 1st order reaction model (shown in Fig. 2). And the 1st order reaction model has also been demonstrated inapplicable for the sublimation of ammonium nitrate [27] and ammonium perchlorate [28]. In these papers, models of contacting cylinder and contracting sphere, which represent two- and three-dimensional phase boundary reaction, are used to describe the kinetics of sublimation process. We believe that sublimation process can be described by the phase boundary reaction model.

The TG–FTIR technique brings us important information about the gaseous products of leucine pyrolysis online, such as the species of gaseous products, their quantities and evolution rate versus time. Although it is difficult to identify every species in the mixture of gas products for the overlapping of their IR absorbance, some gas products with very specific IR absorption, such as CO_2, CO, and NH_3, can be identified easily.

Acknowledgements

This work was financially supported by the National Nature Sciences Foundation of China (Grant No. 20373050), Nature Sciences Foundation of Hubei and China Postdoctoral Science Foundation.

References

[1] C. Merritt, D.H. Robertson, J. Gas Chromatogr. 5 (1967) 96.
[2] W. Simon, P. Kriemler, H. Steiner, J. Gas Chromatogr. 5 (1967) 53.
[3] P.G. Simmonds, E.E. Medley, M.A. Ratcliff, G.P. Shulman, Anal. Chem. 44 (1972) 2060.
[4] M.A. Ratcliff, E.E. Medley, P.G. Simmonds, J. Org. Chem. 39 (1974) 1481.
[5] J.M. Patterson, N.F. Haidar, E.P. Papadopoulos, W.T. Smith, J. Org. Chem. 38 (1973) 663.
[6] G.P. Shulman, P.G. Simmonds, Chem. Commun. 15 (1968) 1040.
[7] N.D. Danielson, L.B. Rogers, Anal. Chem. 50 (1978) 1680.
[8] D. Bougeard, Ber. Bunsenges, Phys. Chem. 87 (1983) 279.
[9] A. Grunenberg, D. Bougeard, B. Schrader, Thermochim. Acta 77 (1984) 59.
[10] F. Rodante, G. Marrosu, Thermochim. Acta 171 (1990) 15.
[11] F. Rodante, G. Marrosu, G. Catalani, Thermochim. Acta 194 (1992) 197.
[12] F. Rodante, Thermochim. Acta 200 (1992) 47.
[13] V.A. Basiuk, J. Anal. Appl. Pyrol. 47 (1998) 127.
[14] J. Douda, V.A. Basiuk, J. Anal. Appl. Pyrol. 56 (2000) 113.
[15] G. Chiavari, D. Fabbri, S. Prati, J. Chromatogr. A 922 (2001) 235.
[16] V.A. Basiuk, J. Douda, Adv. Space Res. 27 (2001) 231.
[17] R.K. Sharma, W.G. Chan, J. Wang, B.E. Waymack, J.B. Wooten, J.I. Seeman, M.R. Hajaligol, J. Anal. Appl. Pyrol. 72 (2004) 153.
[18] S.F. Wang, B.Z. Liu, Q.D. Su, J. Anal. Appl. Pyrol. 71 (2004) 393.
[19] W. Xie, W.P. Pan, J. Therm. Anal. Cal. 65 (2001) 669.
[20] K. Marsanich, F. Barontini, V. Cozzani, L. Petarca, Thermochim. Acta 390 (2002) 153.
[21] M. Webb, P.M. Last, C. Breen, Thermochim. Acta 326 (1999) 151.
[22] C. Breen, P.M. Last, S. Taylor, P. Komadel, Thermochim. Acta 363 (2000) 93.
[23] W.M. Groenewoud, W. de Jong, Thermochim. Acta 286 (1996) 341.
[24] W. Tang, Y. Liu, H. Zhang, C. Wang, Thermochim. Acta 408 (2003) 39.
[25] NIST Chemistry Webbook standard reference database No. 69, June 2005 Release (http://webbook.nist.gov/chemistry).
[26] SADTLER Standard Infrared Vapor Phase Spectra, Sadtler Research Laboratories Inc., 1980.
[27] S. Vyazovkin, J.S. Clawson, C.A. Wight, Chem. Mater. 13 (2001) 960.
[28] P.W.M. Jacobs, A.R. Jones, J. Phys. Chem. 72 (1968) 202.